Int. J. Heat Mass Transfer. Vol. 22, pp. 245–255
0017-9310/79/0201-0245 $02.00/0

ON THE NEAR FIELD CHARACTERISTICS OF AXISYMMETRIC TURBULENT BUOYANT JETS IN A UNIFORM ENVIRONMENT

CHING JEN CHEN* and CONSTANTINOS P. NIKITOPOULOS†
Iowa Institute of Hydraulic Research, Energy Division, The University of Iowa, Iowa City, IA 52242, U.S.A.

Abstract—A differential $k-\varepsilon-\overline{T'^2}$ model is used to investigate the near field characteristics of buoyant jets discharging into a stagnant uniform environment. The lateral temperature and velocity profiles and the half width of turbulent buoyant jets in the zone of flow establishment are calculated. Also the mean centerline velocity and temperature decay, the turbulent kinetic energy and its dissipation rate are computed for a wide range of exit densimetric Froude numbers. A good agreement between the predicted and the available experimental data is obtained. The level of the turbulent fluctuations at the exit is found to have a strong influence on the jet characteristics in the near field region.

NOMENCLATURE

D, exit orifice diameter;
e, basis of the natural logarithm;
F_0, exit densimetric Froude number $= T_a U_{0℄}^2/gD(T_{0℄}-T_a)$;
F_e, densimetric Froude number at the end of the zone of flow establishment $= T_a U_{e℄}^2/2gY_b(T_{e℄}-T_a)$;
g, acceleration of gravity;
k, turbulent kinetic energy $= \overline{u_i u_i}/2$;
$k_℄$, centerline turbulent kinetic energy;
k_0, turbulent kinetic energy at the source;
$k_{0℄}$, centerline kinetic energy at the source;
T, mean jet temperature;
T', fluctuating jet temperature;
T'_0, fluctuating jet temperature at the exit;
T_a, local ambient temperature;
T_0, jet temperature at the exit;
$T_{0℄}$, centerline jet temperature at the exit;
$T_{e℄}$, centerline jet temperature at the end of the ZFE;
$T_℄$, jet centerline temperature;
U, mean jet velocity component in the axial directory;
U_0, mean jet velocity component at the exit;
$U_{e℄}$, mean jet centerline velocity at the end of the ZFE;
$U_{0℄}$, mean jet centerline velocity at the exit;
u, fluctuating velocity component in the x direction $(= u_1)$;
u_i, fluctuating velocity component in the ith direction;
$\overline{u_i u_j}$, turbulent shear stress;
$\overline{u_i T'}$, turbulent heat flux in the ith direction;
V, mean velocity component in the normal direction;
v, fluctuating velocity component in the y direction $(= u_2)$;
x, axial direction of the buoyant jet;
x_e, length of the zone of flow establishment defined in Fig. 1;
x_0, location of the virtual origin;
y, normal direction of the jet from the symmetric axis;
Y_b, distance from the buoyant jet centerline to the point where the velocity is equal to $1/e$ of the centerline velocity;
$y_{0.5U}$, distance from the centerline to the point where the velocity is the half of the centerline velocity;
$y_{0.5T}$, distance from the centerline to the point where the temperature difference $(T-T_a)$ is the half of the temperature difference $(T_℄-T_a)$;
ZFE, zone of flow establishment;
ZEF, zone of established flow.

Greek symbols

ρ, mean jet density;
ρ_a, local ambient density;
ρ_0, density of buoyant jet at the exit;
$\Delta\rho$, $(\rho_a-\rho)$;
ε, dissipation rate of the turbulent kinetic energy;
ε_0, dissipation rate of turbulent kinetic energy at the exit;
$\varepsilon_{0℄}$, centerline dissipation rate of turbulent kinetic energy at the exit;
$\varepsilon_℄$, centerline dissipation rate of turbulent kinetic energy.

Subscripts

a, ambient condition;
b, variable evaluated at Y_b;
℄, centerline value;

*Professor.
†Graduate Research Assistant.

e, at the end of the ZFE;
0, exit condition or the virtual origin (x_0);
$0.5U, 0.5T$, half width of the velocity and temperature respectively;
ent, entrainment;
i,j, respectively equal to 1, 2, 3 denoting x, y and z direction.

I. INTRODUCTION

THE VERTICAL buoyant jet discharging into a uniform stagnant environment is one of the most important flow patterns related with the environmental pollution. Problems associated with the environmental pollution require the knowledge of the buoyant jet characteristics, such as buoyant jet dispersion, decay of centerline velocity, temperature, and behavior of the entrainment velocity.

In the past the prediction of the flow characteristics of the turbulent buoyant jets was most commonly done by employing integral methods. Recently, emphasis is shifted towards the use of differential methods. Although the differential method is more complex than the integral, it has potentially more applications and less restrictions than the integral method. In the integral method, the entrainment rate and the similarity profiles for both the velocity and the temperature must be specified. The differential methods, on the other hand, do not employ profiles and entrainment assumptions but they obtain the profiles and the entrainment rate as part of the solution.

In general, the differential method is constituted by the partial differential equations governing the mean velocity and temperature components, and the turbulent momentum and energy fluxes. Since the resulting set of equations has more unknowns than it can accommodate, assumptions about the turbulent transport processes are introduced. These assumptions form a turbulence model. The accuracy of the differential method thus depends on the turbulence model used.

Many turbulence models for the prediction of turbulent buoyant and non-buoyant jets are available in the literature. Madni and Pletcher [1] in their analysis used a mixing length model. Higher order closure models were proposed by Launder [2], Lumley [3], Donaldson *et al.* [4], Mellor [5], Mellor and Yamada [6], Meroney [7], Lumley and Khajeh-Nouri [8] and many others. Donaldson *et al.* [4] and Meroney [7] applied their models to the problem of the clear air turbulence; Mellor [5] used in studying boundary stratified layers; Gibson and Launder [9] tested Launder's [2] model by applying it to horizontal surface jets and mixing layers. Chen and Rodi [10] modified Launder's model to predict the far field region characteristics of buoyant turbulent jets discharging into a uniform or stratified environment.

In this investigation, a turbulence model, proposed by Chen and Rodi [10] is used: (1) to investigate the behavior of axisymmetric buoyant jets in the near field region; (2) to examine the effect of the exit turbulent intensity on the developing buoyant jet core; (3) to compute the rates of spread of turbulent jets and other flow variables under different exit conditions; (4) to demonstrate the applicability of the differential method in cases where an integral method fails to give accurate predictions.

II. ANALYSIS AND TURBULENT MODEL

Figure 1 depicts a vertical buoyant jet discharged into a uniform stagnant environment from an exit with a finite diameter D. As the buoyant jet advances, it passes first from a region called the zone of flow establishment (ZFE) which extends to about 10 diameters downstream from the source. It is in

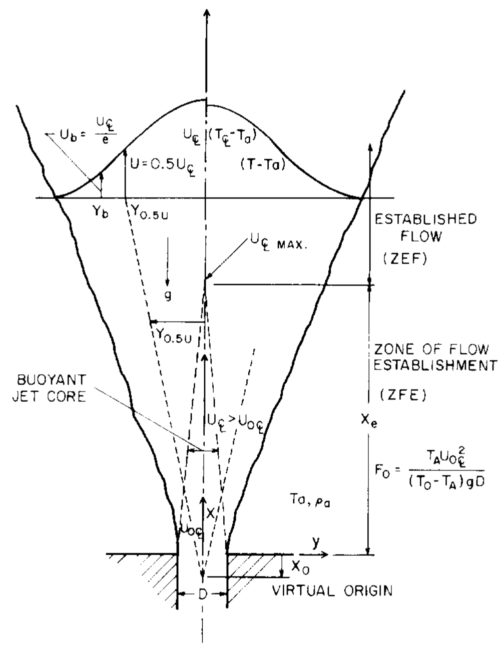

FIG. 1. Sketch of an axi-symmetric buoyant jet in a uniform stagnant environment.

this region that the jet fluid begins to mix with the ambient fluid. A shear layer is developed at the edge of the jet, and as the jet advances this layer is dispersed toward the jet axis. When the shear layer reaches the symmetry axis, the flow is said to be established. The region from the source to the point where the central line velocity begins to decay from a maximum value is called the zone of flow establishment. Beyond this point the flow enters the zone of established flow (ZEF). Under the assumptions that the flow is steady and of the boundary-layer type (i.e. $U \gg V$, $\partial/\partial y \gg \partial/\partial x$), and employing the Boussinesq approximation, in which the density variation is accounted for only in the gravitational term, the governing equations for the velocity and temperature are:

conservation of mass

$$\frac{\partial U}{\partial x} + \frac{1}{y}\frac{\partial}{\partial y}(yV) = 0 \tag{1}$$

conservation of momentum

$$U\frac{\partial U}{\partial x}+V\frac{\partial U}{\partial y}=\frac{1}{y}\frac{\partial}{\partial y}(-y\overline{uv})+g\frac{T-T_a}{T_a} \quad (2)$$

conservation of energy

$$U\frac{\partial T}{\partial x}+V\frac{\partial T}{\partial y}=\frac{1}{y}\frac{\partial}{\partial y}(-y\overline{vT'}) \quad (3)$$

where x and y are the axial and the normal direction of the buoyant jet, and U and V are the corresponding velocity components and T_a is the ambient mean temperature. The last term of equation (2) is the buoyancy term resulting from the Boussinesq approximation. The two turbulent quantities $\overline{uv}$ and $\overline{vT'}$ are the turbulent shear stress and heat flux respectively. The viscous and conductive term in equations (2) and (3) are neglected since they are small compared with the turbulent stress and heat flux. In order to solve equations (1)–(3), a turbulence closure model for the turbulent stresses and heat fluxes has to be specified. In this study, the model proposed by Chen and Rodi [10] is adopted. This model is based on closure approximations made in the turbulent transport equations for the turbulent shear stress $\overline{u_iu_j}$, the dissipation rate of turbulent kinetic energy, k, $(k=\frac{1}{2}\overline{u_iu_i})$, ε, $\left(\varepsilon=\nu\overline{\frac{\partial u_i}{x_k}\frac{\partial u_i}{\partial x_k}}\right)$, the turbulent heat flux $\overline{u_iT'}$, and the fluctuating temperature $\overline{T'^2}$. This model is termed briefly as the $k-\varepsilon-\overline{T'^2}$ model. The subscript i and j stand for 1, 2, 3 denoting the x, y and z components of fluctuating velocity u_i. In the case of the repeated subscripts the Cartesian tensor summation convention applies. The differential equations for the $k-\varepsilon-\overline{T'^2}$ model under the boundary-layer approximation are given as [10]

Convection	Diffusion	Production	Dissipation	
$U\frac{\partial k}{\partial x}+V\frac{\partial k}{\partial y}$	$=\frac{1}{y}\frac{\partial}{\partial y}\left(yc_k\frac{k\overline{v^2}}{\varepsilon}\frac{\partial k}{\partial y}\right)$	$-\ \overline{uv}\frac{\partial U}{\partial y}+\frac{\overline{guT'}}{T_a}$	$-\ \varepsilon$	(4)
$U\frac{\partial \varepsilon}{\partial x}+V\frac{\partial \varepsilon}{\partial y}$	$=\frac{1}{y}\frac{\partial}{\partial y}\left(yc_\varepsilon\frac{k\overline{v^2}}{\varepsilon}\frac{\partial \varepsilon}{\partial y}\right)$	$+\ c_{\varepsilon1}\frac{\varepsilon}{k}\left(-\overline{uv}\frac{\partial U}{\partial y}+\frac{\overline{guT'}}{T_a}\right)$	$-\ c_{\varepsilon2}\frac{\varepsilon^2}{k}$	(5)
$U\frac{\partial\overline{T'^2}}{\partial x}+V\frac{\partial\overline{T'^2}}{\partial y}$	$=\frac{1}{y}\frac{\partial}{\partial y}\left(yc_T\frac{k^2}{\varepsilon}\frac{\partial\overline{T'^2}}{\partial y}\right)$	$-\ 2\overline{vT'}\frac{\partial T}{\partial y}$	$-\ c_{T1}\frac{\varepsilon\overline{T'^2}}{k}.$	(6)

The term on the LHS of equations (4) and (6) represent the convection of k, ε, and $\overline{T'^2}$ respectively. The first term on the RHS of these equations can be interpreted as the diffusive contribution of the respective variables. The second term is the production and the third is the dissipation of k, ε, and $\overline{T'^2}$ respectively. The term $\overline{guT'}/T_a$ appeared in equations (4) and (5) is the buoyant contribution to the turbulent transport process of k, ε and $\overline{T'^2}$.

The differential equations for the Reynolds stresses and the heat fluxes, $\overline{u_iu_j}$ and $\overline{u_iT'}$, which include the $\overline{uv}$ and $\overline{vT'}$ terms appeared in equations (2) and (3) are given by Hossain and Rodi [11]. In the present investigation these equations are simplified by neglecting respectively the convective and diffusive transport terms of $\overline{u_iu_j}$ and $\overline{u_iT'}$. This leads to the following approximated algebraic relations for the $\overline{uv}$, $\overline{v^2}$, $\overline{vT'}$ and $\overline{uT'}$ terms

$$-\overline{uv}=\frac{1-c_0}{c_1}\frac{\overline{v^2}}{k}\left[1+\frac{kg\dfrac{\partial T}{\partial y}}{c_h\varepsilon T_a\left(\dfrac{\partial U}{\partial y}\right)}\right]\frac{k^2}{\varepsilon}\frac{\partial U}{\partial y} \quad (7)$$

$$\overline{v^2}=c_2k \quad (8)$$

$$-\overline{vT'}=\frac{1}{c_h}\frac{\overline{v^2}}{k}\frac{k^2}{\varepsilon}\frac{\partial T}{\partial y} \quad (9)$$

$$\overline{uT'}=\frac{k}{c_h\varepsilon}\left[-\overline{uv}\frac{\partial T}{\partial y}-\overline{vT'}(1-c_{h1})\frac{\partial U}{\partial y}+\frac{g(1-c_{h1})}{T_a}\overline{T'^2}\right]. \quad (10)$$

Equations (1)–(10) form the $k-\varepsilon-\overline{T'^2}$ turbulent model containing 11 empirical constants. These constants are determined and calibrated with data from many turbulent flow measurements and are shown, for example, by Hanjalic and Launder [12] and others to be approximately constants. We adopt the same constant values proposed by Chen and Rodi [10] as follows.

C_0	C_1	C_2	C_ε	$C_{\varepsilon 1}$	$C_{\varepsilon 2}$	C_k	C_T	C_{T1}	C_h	C_{h1}
0.55	2.2	0.53	0.15	1.43	1.92	0.225	0.13	1.25	3.2	0.5

We also adopt a correction function as suggested by Chen and Rodi [10]. According to them the RHS of equation (7) is multiplied by $(1-0.465G)$ and $c_{\varepsilon 2}$ is multiplied by $(1-0.035G)$ where

$$G = \left|\frac{y_{0.5U}}{2U_{\mathbb{C}}}\left(\frac{\mathrm{d}U_{\mathbb{C}}}{\mathrm{d}x} - \left|\frac{\mathrm{d}U_{\mathbb{C}}}{\mathrm{d}x}\right|\right)\right|^{0.2}. \tag{11}$$

Here $y_{0.5U}$ is the half-jet width and the subscript $\mathbb{C}$ denotes the centerline value. The governing equations (1)–(11) form a parabolic system and are solved by Patankar and Spalding's [13] finite difference procedure modified to adopt the present turbulence model.

III. BOUNDARY AND EXIT CONDITIONS

We specify boundary conditions at the edge and the axis of a buoyant jet as follows

$$x>0 \quad y \to \infty \quad T=T_a \quad U=k=\varepsilon=\overline{T'^2}=0$$

$$x>0 \quad y=0 \quad \frac{\partial}{\partial y}\ [T, U, k, \varepsilon, \overline{T'^2}] = 0. \tag{12}$$

At the beginning of the computation, the exit mean velocity and temperature profiles, the turbulent kinetic energy k_0, its dissipation rate ε_0 and the temperature fluctuation $\overline{T_0'^2}$ must be prescribed. It was decided to calculate a flat and a triangular profile for both the exit mean velocity and temperature. One may consider the flat profile as an approximation for the flow issuing from a cooling tower or the flow generated behind a uniform grid. The triangle profile is chosen because it resembles closely the developed profile. Calculations are made for both profiles so that the effect of initial mean profile on the flow characteristics, in the ZFE and more generally in the near field, can be examined.

The literature on experimental measurements did not provide the profiles for the initial turbulent kinetic energy k_0 (or the level of turbulent intensity), its dissipation function ε_0 and the temperature fluctuation $\overline{T_0'^2}$. In the present study, Gaussian profiles were assumed for k_0, ε_0 and $\overline{T_0'^2}$. These profiles are:

$$x=0 \left\{ \begin{array}{l} k_0 = k_{0\mathbb{C}}\ \exp(-1.7y^2) \\ \varepsilon_0 = \varepsilon_{0\mathbb{C}}\ \exp(-1.7y^2) \\ \overline{T_0'^2} = \overline{T_{0\mathbb{C}}'^2}\ \exp(-1.7y^2) \end{array} \right\} 0 \leqslant y \leqslant \frac{D}{2} \tag{13}$$

where the centerline value of k, ε, and $\overline{T'^2}$ at the exit are denoted by $k_{0\mathbb{C}}$, $\varepsilon_{0\mathbb{C}}$, and $\overline{T_{0\mathbb{C}}'^2}$. They are given as percentage fractions of the U_0^2, U_0^3/D and $(T_0-T_a)^2$ respectively in the calculation.

IV. RESULTS AND DISCUSSIONS

Calculations were made for buoyant and non-buoyant jets. For the case of buoyant jets, calculations for a wide range of exit densimetric Froude numbers (1–625) where performed. A typical calculation requires approximately 4 min of IBM 360 time to cover the region from the exit to about 25 diameter downstream in 450 steps.

IV.1. *Exit turbulent level and the zone of flow establishment*

The effects of the initial turbulent level on the length of the ZFE and on the centerline velocity development are shown in Figs. 2 and 3 respectively. The length of ZFE, x_e, is taken as the distance from the exit to the location where the maximum axial velocity starts to decay. For a non-buoyant jet the maximum axial velocity in the ZFE is equal to the exit velocity. However, for a buoyant jet the flow is accelerated by the buoyancy force before it starts decaying (see Fig. 7). Therefore, the maximum axial velocity in the ZFE in general is equal or larger than the exit velocity, $U_{0\mathbb{C}}$. Figure 2 shows the plot of the length of ZFE as a function of the initial turbulent level, $k_{0\mathbb{C}}/U_{0\mathbb{C}}^2$. It is observed that generally the higher the initial turbulent level is, the shorter the length of the ZFE becomes. Figure 2 also shows that the length of the ZFE for a low turbulence level, say $K_{0\mathbb{C}}/U_{0\mathbb{C}}^2 = 10^{-3}$, may be 2 or 3 times larger than the length of the ZFE at a higher turbulence level, say $k_{0\mathbb{C}}/U_{0\mathbb{C}}^2 = 10^{-1}$. From the figure it is observed that the effect of the buoyancy is to decrease the length of the ZFE. As the turbulence level is reduced the length of the ZFE approaches an asymptotic value. For non-buoyant jets the limiting length of the ZFE, x_e/D, is about 8 and for plumes is about 7. It was found that the axial temperature and velocity start to decay at approximately the same location. Therefore no specific distinction of the ZFE for the temperature and the velocity is made.

In order to fix a turbulent level for the subsequent calculations, the predicted length of the ZFE based on a flat initial profile at different initial turbulence levels, was compared with the experimental data of Albertson *et al.* [14] as shown in Fig. 3. The figure showed that the predicted solution, based on the initial turbulence level of 1.25% ($k_{0\mathbb{C}}/U_{0\mathbb{C}}^2 = 0.0125$), compares most closely with the experimental data. This turbulence level is then adopted in all subsequent calculations.

IV.2. *Development of lateral profiles*

Figures 4 and 5 give the development of the lateral velocity and temperature profiles for the case of $F_0 = 9$ respectively with the flat and triangular exit

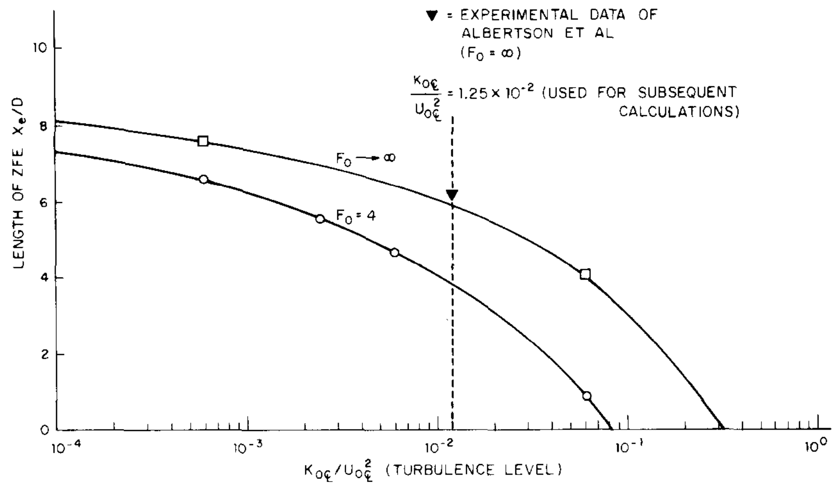

FIG. 2. Influence of the exit turbulent level on the length of the zone of flow establishment.

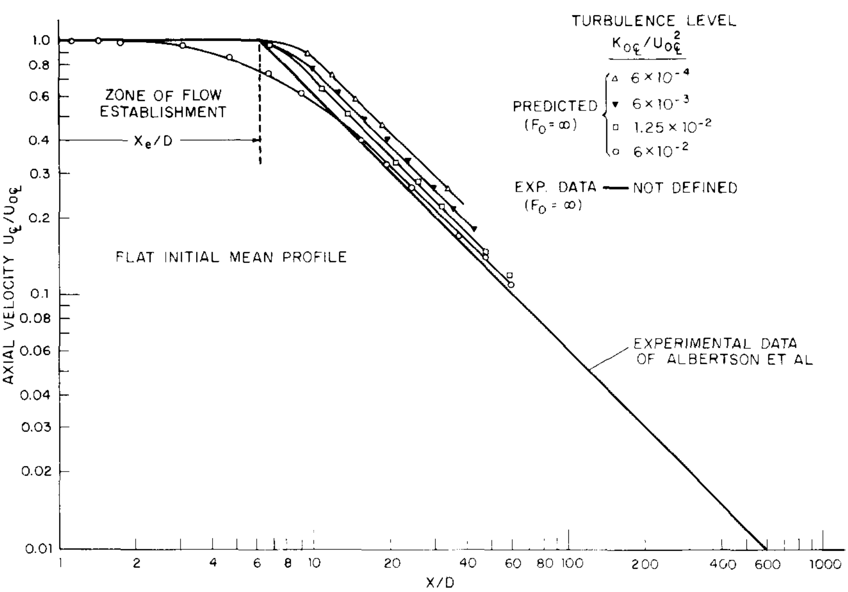

FIG. 3. Effect of the exit turbulent level on the decay of the centerline velocity.

mean profiles. In these plots the velocity and temperature are normalized by the local centerline values while the radial coordinate is normalized by the local half width $y_{0.5U}$. $y_{0.5U}$ is the radial location at which the velocity is one-half of the centerline velocity.

Figure 4 shows the development of the lateral profiles for the case of flat initial profile. It was observed that at approximately 5 diameters from the source the profile is almost developed. In the case of the triangular initial profile, the flow needs only one or two diameters to become almost developed, as shown in Fig. 5. The velocity and temperature measured by Nakagome and Hirata [15] for $F_0 = 0$ at $x/D > 4$ is also included in Figs. 4 and 5. Good agreement is obtained between the computed and the experimental results.

IV.3. *Virtual origin*

The "virtual origin" of a buoyant jet may be defined as the apex of the cone of the half-width $Y_{0.5U}$. From the discussion of Figs. 2–5 we observe that the length of ZFE depends not only on the initial turbulence level but also on the exit mean velocity and temperature profiles. The length of the ZFE obviously affects the location of the virtual origin, since a change of this length causes the beginning of the ZFE to move further or closer to the exit. Therefore, the virtual origin depends on the exit mean profiles, the turbulence level and the buoyant force (i.e. Froude number). Chen and Rodi [16] found from the available experiment data that the virtual origins for all buoyant jets, including non-buoyant ones, are located somewhere between three diameters inside and outside of the jet exit. From

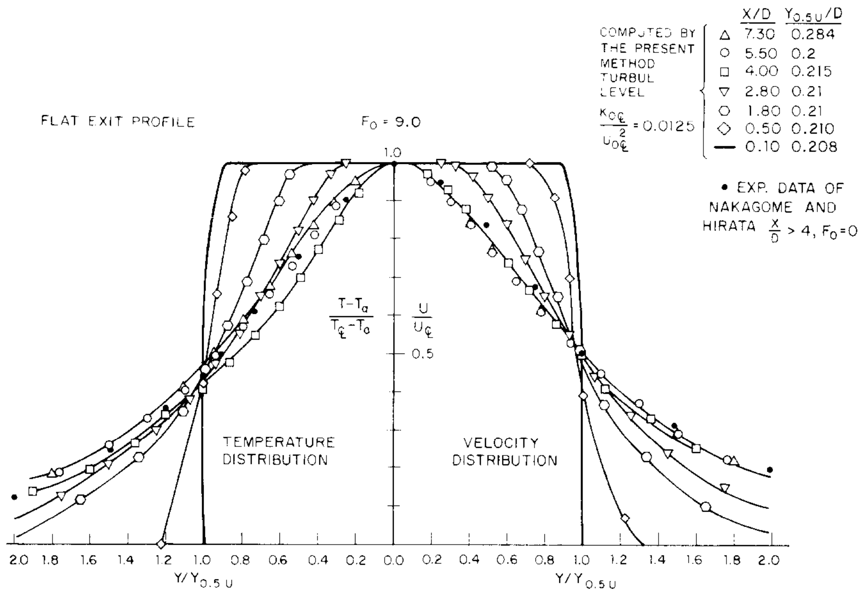

FIG. 4. Development of the velocity and temperature profiles in the ZFE for initially flat mean profile.

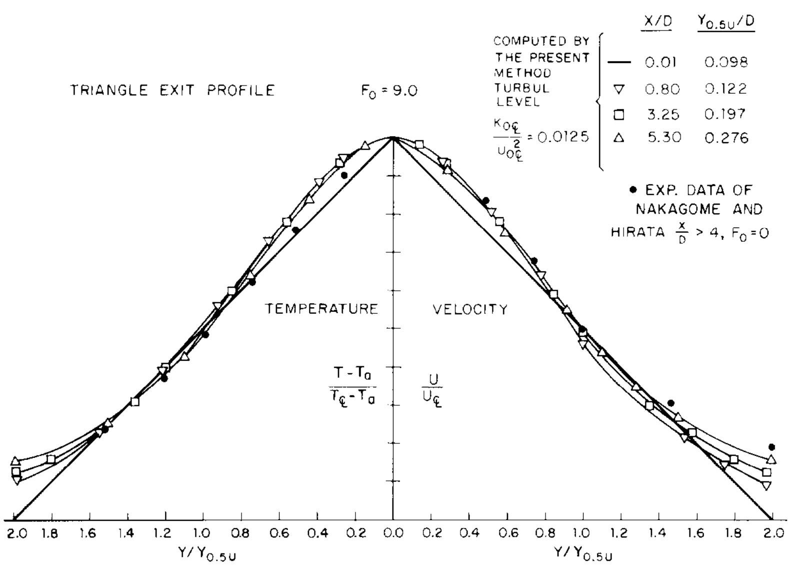

FIG. 5. Development of the velocity and temperature profiles in the ZFE for initially triangular mean profile.

Figs. 2–5 we may conclude that a combination of the flat initial profile, a large exit Froude number and a low turbulence level contribute to move the virtual origin up along the axis. The combination of the triangle profile, a small exit Froude number and a high turbulence level contribute to move the virtual origin backward along the axis. In Fig. 6 the velocity half-width, $Y_{0.5U}/D$, is plotted as a function of the axial location x/D, for the case of flat initial velocity and temperature profiles. For the case of the buoyant jet with $F_0 = 64$ two separate computations were performed. One with $k_{0\mathbb{C}}/U_{0\mathbb{C}}^2 = 0.0125$ and another with $k_{0\mathbb{C}}/U_{0\mathbb{C}}^2 = 0.06$. The former calculation ($k_{0\mathbb{C}}/U_{0\mathbb{C}}^2 = 0.0125$) shows that the location of the virtual origin is at approximately 1.5 diameters downstream from the exit (i.e. at $x_0/D = 1.5$). The latter calculation ($k_{0\mathbb{C}}/U_0^2 = 0.06$) shows that the virtual origin has been moved upstream at $x_0/D = -1.5$.

IV.4. *Development of half-width*

In Fig. 6, the predicted velocity half-width as well as the exponential width Y_b are plotted. As shown in Fig. 1 the exponential width Y_b is defined as the radial distance from the centerline jet axis to the point where the velocity is equal to $1/e$ of the corresponding centerline velocity. Here e is the basis of the natural logarithm.

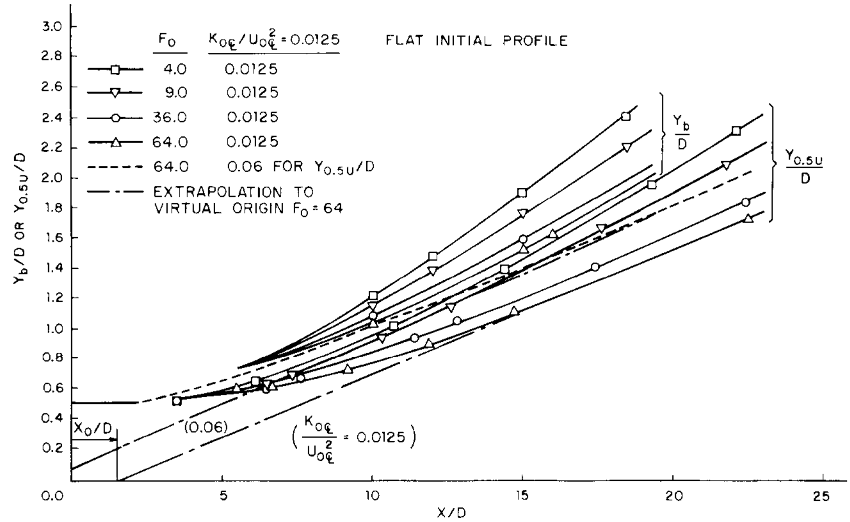

FIG. 6. Velocity half-width and exponential width.

From Fig. 6 it becomes evident that the rates of spread $dY_{0.5U}/dx$ and dY_b/dx are large for small exit densimetric Froude numbers. This is in accordance with the conclusions of the survey of the available experimental data made by Chen and Rodi [16]. The present calculation of the rate of the half-width spread is compared in Table 1 with the most reliable data recommended by Chen and Rodi [16]. The half-width for velocity and temperature spread $dY_{0.5U}/dx$ and $dY_{0.5T}/dx$ are calculated for both flat and triangular exit profiles. Listed in Table 1 the predicted values of the rate of spreads are taken at approximately 25 diameters downstream from the jet exit. The difference between the experimental and predicted values is within 10%.

From Table 1 one sees that the rate of spread $dY_{0.5T}/dx$ is not sensitive to Froude number, F_0, while the rate of spread $dY_{0.5U}/dx$ is. This is because the buoyancy force directly appears in momentum equation (2) but indirectly affects the temperature profile through convective term in energy equation (3). In addition, the Reynolds stress term $\overline{uv}$ that appears in equation (2) is modeled by equation (7) which contains the buoyant force explicitly. On the other hand, the heat flux term $\overline{UT'}$ that appears in equation (3) is modeled by equation (9) which does not explicitly contain the buoyant force. In investigating plane buoyant jets Chen and Rodi [16] reported similar insensitivity of the rate of spread $dY_{0.5T}/dx$ to the Froude number. They gave the temperature spreading rate $dY_{0.5T}/dx$ of 0.14 for plane non-buoyant jet and 0.13 for plane plume. However, the velocity spreading rate $dY_{0.5U}/dx$ of 0.11 for plane non-buoyant jet and 0.135 for plane plume are predicted.

IV.5. *Variation of centerline velocity and temperature*

Figures 7 and 8 present the variation of the axial velocity and temperature respectively, for a wide range of densimetric Froude numbers. In Fig. 7, the centerline velocity of four buoyant jets ($F_0 = 4$, 9, 36, 100) is plotted vs the longitudinal distance. It is shown that at low exit densimetric Froude numbers, the acceleration due to the buoyancy force is more pronounced than for the case of high exit densimetric Froude numbers. For $F_0 = 4$, the centerline velocity the ZFE attains a value of $1.7U_{0\mathbb{C}}$, while for the case of $F_0 = 100$, the centerline velocity in the ZFE is shown to be constant and equal to its exit value. This comparison indicates that the effect of the buoyancy force in the ZFE should not be ignored as is commonly done in the case of the integral method approach. Thus for flows with low Froude number the initial conditions for the integral method should be taken for the ones at the beginning of the ZFE which are predicted by the present differential method. Figure 7 also gives the behavior of the local

Table 1. Comparison of experimental and numerical results of the rate of spread for non-buoyant and buoyant jets

	Buoyant jet $F_0 = 0$ (Plume)		Non-buoyant jet	
	$dY_{0.5U}/dx$	$dY_{0.5T}/dx$	$dY_{0.5U}/dx$	$dY_{0.5T}/dx$
Experiment	0.112	0.104	0.086	0.11
pred. (flat)*	0.105	0.106	0.084	0.107
pred. (triangle)*	0.110	0.112	0.091	0.112

*Taken at $x/D = 25$, initial turbulence level $k_{0\mathbb{C}}/U_{0\mathbb{C}}^2 = 0.0125$.

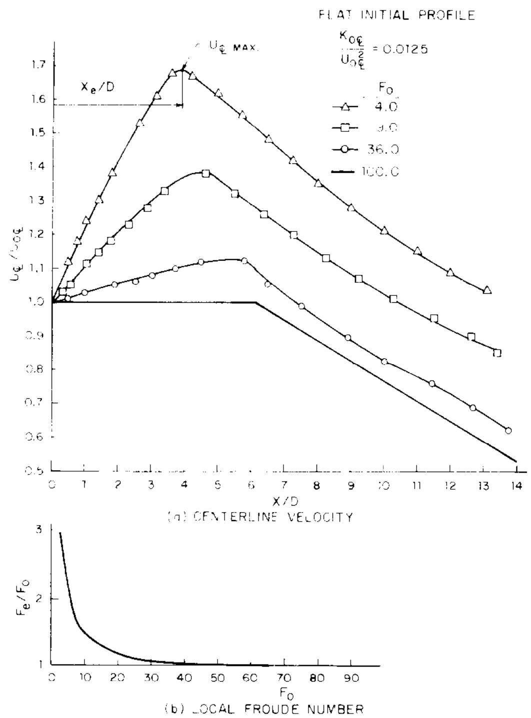

FIG. 7. Development of the centerline velocity and the local Froude number.

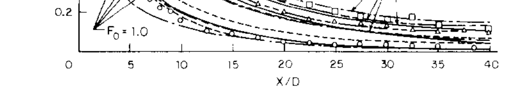

FIG. 8. Comparison of experimental data and theoretical results.

Froude number at the end of the zone of flow establishment as a function of the exit Froude number F_0. The local Froude number at the end of the ZFE is defined as

$$F_e = \frac{U_{℄e}^2}{g2Y_b \dfrac{T_{e℄} - T_a}{T_a}}.$$

It is concluded that only when the exit Froude number is more than, say, 64 the buoyant acceleration of the axial velocity can be considered negligible. Thus in applying the integral method to solve buoyant flows, the F_e rather than F_0 should be used as the initial condition for the equations describing the flow since the similarity of the axial velocity and temperature decay begins at the start of the ZFE. Figure 8 compares the temperature centerline decay predicted by the present method, Madni and Pletcher [1], Pryputniewicz [17] and Trent [18] with the experimental data of Pryputniewicz [17]. The comparison shows that the present differential method and Madni and Pletcher mixing length Model [1] give much more accurate predictions than the integral method of Trent [18] and Pryputniewicz [17]. The results of Hirst's [19] integral method, although not shown in Fig. 8, were found inaccurate, particularly at low exit densimetric Froude numbers. The present $k-\varepsilon-\overline{T'^2}$ model gives somewhat better results than Madni and Platcher [1] mixing length model for both the near and far held regions. Further results for the far field region are given by Chen and Chen [20].

IV.6. *Turbulent kinetic energy and its dissipation function*

Although the turbulent transport properties may not have direct industrial applications, they always reveal how the turbulent processes affect and modify the flow pattern. Here two important quantities are discussed namely the turbulent kinetic energy, k, and its dissipation function ε. The turbulent energy denotes the energy content of the fluctuating velocity available for turbulent transport processes other than the molecular means. The turbulent dissipation controls the growth of the turbulence energy. In Figs. 9 and 10 the variation of the centerline turbulent kinetic energy $k_℄$ normalized by $U_{0℄}^2$ and its dissipation function $\varepsilon_℄$ normalized by $U_{0℄}^3/D$ are plotted respectively. From Fig. 9 one observes that the kinetic energy immediately after the jet's exit starts decaying, and after reaching a minimum value it starts amplifying again. The point where the kinetic energy attains its minimum value moves downstream from the source, as the exit densimetric Froude number increases. The decrement of the turbulent kinetic energy next to the exit region can be explained as the following: The velocity profile in the ZFE near the axis remains flat so that, the turbulent kinetic energy production by shear strain

$$\left(-\overline{u_i u_j}\frac{\partial U}{\partial y}\right)$$

is not possible; and the turbulent kinetic energy production from buoyant force is also small, since $\overline{uT'}$ as shown in equation (10) depends on the turbulent kinetic energy. Under these conditions the turbulent flow decays. When the shear layer develops and reaches eventually the jet centerline the turbulent production by the shear strain and buoyancy force permits the turbulent kinetic energy to grow again. However, when the flow reaches the established zone it eventually will decay. In Fig. 9 the behavior of the centerline turbulent kinetic energy of a buoyant jet with $F_0 = 64$, under two different initial values of the turbulent kinetic energy, $k_{0℄}/U_0^2 = 0.0125$ and 0.06, is plotted. In both cases, the centerline turbulent kinetic energy shows the same behavior. It decreases, reaches a minimum value and

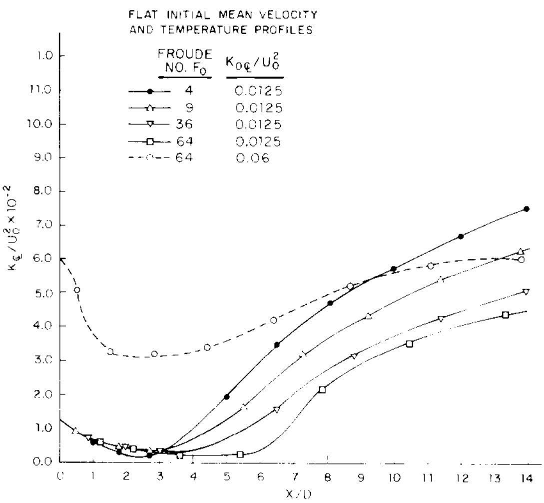

FIG. 9. Development of the centerline turbulent kinetic energy.

then starts increasing again although their location of the minimum is different. Chen and Chen [20] reported that after about 60 diameters downstream from the source the turbulent transport properties will become similar for both cases. Considering the distance required for the velocity and temperature profiles to become similar which is about 10 diameters downstream from the source, one can conclude from Fig. 9 that the process of the turbulent properties to become similar is much slower than the corresponding process for the mean velocity and temperature.

Figure 10 shows the corresponding development of the centerline turbulent dissipation function. It has the same trend as the turbulent kinetic energy i.e. to decay first and then to amplify. The physical mechanism for producing the dissipation is also

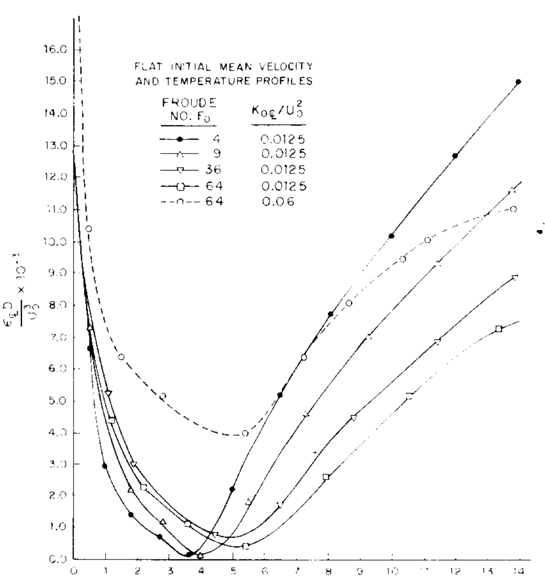

FIG. 10. Development of the centerline turbulent dissipation function.

similar to that of the turbulent kinetic energy. This can be seen from equation (5) that the production of ε is shown to be proportional to the production of k. It is noted from Figs. 9 and 10 that the amplification of the centerline dissipation function $\varepsilon_{℄}$ and the turbulent kinetic energy after its initial decay does not recover its initial exit value for $k_{0℄}/U_0^2 = 0.06$.

IV.7. *Entrainment*

Figure 11 presents the behavior of the entrainment velocity, V_{ent}, of a buoyant jet, for a region covering up to about 15 diameters downstream from the jet exit. The entrainment velocity is normalized by the local centerline velocity $U_{℄}$. It is shown that the smaller the exit densimetric Froude number, the larger the non-dimensional entrainment velocity,

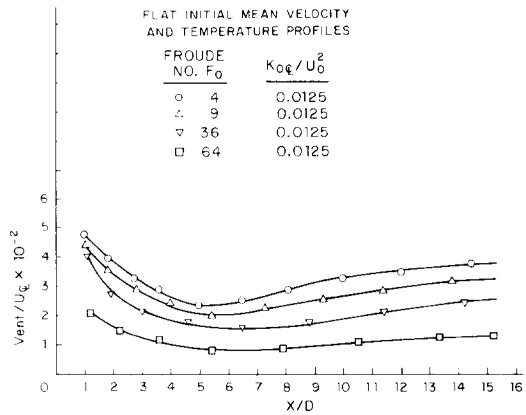

FIG. 11. Behavior of the entrainment velocity in the near field.

$V_{ent}/U_{℄}$. The normalized $V_{ent}/U_{℄}$ starts decaying immediately after the jet exit. It reaches a minimum level and then starts increasing. The decrement of the normalized V_{ent} in the ZFE is due to the increment of the local centerline velocity $U_{℄}$ rather than to the absolute decrement of V_{ent} itself. As the centerline velocity starts decaying in the ZEF, the normalized entrainment velocity starts increasing constantly.

V. CONCLUSIONS

The turbulent model suggested by Chen and Rodi [10] is used herein to study the near field characteristics of buoyant turbulent jets discharged into a stagnant uniform environment. The predicted centerline velocities and temperatures are in good agreement with available experimental results when the turbulent quantities k, ε, and $\overline{T'^2}$ as well as the mean velocity and temperature profiles at the exit are properly prescribed.

Also in the near field region predicted are (1) the location of the virtual origin, (2) the length of the ZFE, (3) the centerline temperature and velocity behavior, (4) the lateral temperature and velocity profiles, (5) the half width of the jet, (6) the local Froude number, (7) the axial variation of the turbulent kinetic energy and the dissipation function of that energy, and (8) the entrainment velocity. The predictions show that the flow variables in the near field are strongly dependent on the initial conditions and on the buoyancy force.

The length of ZFE for the triangle initial profile is considerably shorter than that for the flat initial profile.

REFERENCES

1. I. K. Madni and R. H. Pletcher, Prediction of turbulent forced plumes issuing vertically into stratified or uniform ambients, *J. Heat Transfer* **99**(1), 99–104 (1976).
2. B. E. Launder, Turbulence model and their experimental verification, Imperial College, Dept. of Mechanical Engineering Report HTS/73/26 (1973).
3. J. L. Lumley, A model for computation of stratified turbulent flows, *Int. Symposium on Stratified Flows*, Novosibirsk (1972).
4. D. P. Donaldson, R. D. Sullivan and H. Rosenbaum, A theoretical study of the generation of atmospheric clear air turbulence, *AIAA Jl* **10**(2), 162–170 (1972).
5. G. L. Mellor, Analytical prediction of the properties of stratified planetary surface layers, *J. Atmos. Sci.* **30**(6), 1061–1069 (1973).
6. G. L. Mellor and T. Yamada, A hierarchy of turbulent closure models for planetary boundary layers, *J. Atmos. Sci.* **31**, 1791–1806 (1974).
7. R. N. Meroney, Buoyancy effects on a turbulent shear flow, Project THEMIS Rep. No. 28, Colorado State University (1974).
8. J. L. Lumley and B. Khajeh-Nouri, Computational modeling of turbulent transport, in *Turbulent Diffusion in Environmental Pollution*, edited by F. N. Frenkiel and R. E. Munn. Academic Press, New York (1974).
9. M. M. Gibson and B. E. Launder, On the calculation of horizontal nonequilibrium turbulent shear flows under gravitational influence, *J. Heat Transfer* **98**, 81–87 (1976).
10. C. J. Chen and W. Rodi, A mathematical model for stratified turbulent flow and its application to buoyant jets, *16th IAHR Congress*, Section C.a, San Paulo, Brazil (1975).
11. M. S. Hossain and W. Rodi, Equations for turbulent buoyant flows and their modeling, Rep. SFB 80/T/46, Unviersity of Karlstruhe (1974).
12. K. Hanjalic and B. E. Launder, A Reynolds stress model of turbulence and its application to thin shear flows, *J. Fluid Mech.* **52**, 609–638 (1972).
13. S. W. Patankar and D. B. Spalding, *Heat and Mass Transfer in Boundary Layers*. Intext, London (1970).
14. M. L. Albertson, Y. B. Dai, R. A. Jensen and H. Rouse, Diffusion of Submerged Jets, *Trans. Am. Soc. Civ. Engrs.*, **74**, 639–664 (1948).
15. H. Nakagome and M. Hirata, The Structure of Turbulent Diffusion in an Axi-Symmetrical Thermal Plume, in *Proceedings of International Center for Heat and Mass Transfer*, Seminar on Turbulent Buoyant Convection, Dubrovnik, Yugoslavia, pp. 365–372 (1976).
16. C. J. Chen and W. Rodi, A review of experimental data of vertical turbulent buoyant jets, Report 193 Iowa Institute of Hydraulic Research, The University of Iowa, Iowa City, Iowa, October, 1976. To be published in *Heat and Mass Transfer Series*. Pergamon Press, Oxford.
17. R. J. Pryputniewicz, An experimental study of the free surface effects and submerged vertical buoyant jet, M.S. Thesis, University of Connecticut (1974).
18. P. S. Trent and J. R. Welty, Numerical computation of momentum jets and force plumes, in *Computers and Fluids*, Vol. 1, pp. 331–357. Pergamon Press, New York, (1973).
19. E. Hirst, Buoyant jets with three-dimensional trajectories, *J. Hydraul. Div., Am. Soc. Civ. Engrs*, **98**, (HY11), 1999–2019 (1972).
20. C. J. Chen and C. H. Chen, On prediction and unified correlation for decay of vertical buoyant jets, Paper 78-HT-21, *2nd AIAA/ASME Thermophysics and Heat Transfer Conference*, Palo Alto, California, 24–26 May (1978).

SUR LES CARACTERISTIQUES DE CHAMP PROCHE DE JETS TURBULENTS AXISYMETRIQUES EN CONVECTION NATURELLE DANS UN ENVIRONMENT UNIFORME

Résumé—On utilise un modèle différentiel $k-\varepsilon-\overline{T'^2}$ pour étudier les caractéristiques de champ proche de jets qui évoluent en convection naturelle dans un environment uniforme et au repos. On calcule les profils latéraux de température et de vitesse ainsi que la demi-largeur des jets turbulents dans la zone d'établissement de l'écoulement. De même, on détermine, pour un large domaine de nombre de Froude à la sortie, la décroissance axiale de la vitesse et de la température, l'énergie cinétique turbulente et son taux de dissipation. On obtient un bon accord entre le calcul et les données expérimentales disponibles. On trouve que le niveau des fluctuations turbulentes à la sortie influence fortement les caractéristiques du jet dans la région de champ proche.

DIE NAHFELD-EIGENSCHAFTEN ACHSENSYMMETRISCHER TURBULENTER FREISTRAHLEN MIT AUFTRIEBSEINFLUß IN EINER GLEICHFÖRMIGEN UMGEBUNG

Zusammenfassung—Ein differentiales $k-\varepsilon-\overline{T'^2}$—Modell wird zur Untersuchung der Nahfeld—Eigenschaften von Freistrahlen mit Auftriebseinfluß, die in eine ruhende gleichförmige Umgebung einströmen, verwendet. Die Temperatur—und Geschwindigkeitsprofile und die halbe Breite der Freistrahlen im Gebiet der ausgebildeten Strömung werden berechnet. Ebenso werden die mittlere Kerngeschwindigkeit, der Temperaturabfall, die turbulente kinetische Energie und ihre Dissipationstrate für einen großen Bereich von mit der Dichte gebildeten Austritts-Froude-Zahlen berechnet. Zwischen den berechneten und den verfügbaren experimentellen Werten wird gute Übereinstimmung erreicht. Das Niveau der turbulenten Fluktuationen am Austritt hat, wie sich zeigt, einen großen Einfluß auf die Strahleigenschaften im Gebiet des Nahfeldes.

О ХАРАКТЕРИСТИКАХ БЛИЖНЕГО ПОЛЯ ОСЕСИММЕТРИЧНЫХ ТУРБУЛЕНТНЫХ СВОБОДНОКОНВЕКТИВНЫХ СТРУЙ В ОДНОРОДНОЙ ОКРУЖАЮЩЕЙ СРЕДЕ

Аннотация — Для исследования характеристик ближней зоны свободноконвективных струй, истекающих в неподвижную однородную окружающую среду, используется дифференциальная $k - \varepsilon - T'^2$ модель. Рассчитываются поперечные профили температуры и скорости, а также полуширина турбулентных свободноконвективных струй в зоне развития течения. Кроме того, определяется затухание средних значений скорости и температуры на оси струи, рассчитывается турбулентная кинетическая энергия и скорость её диссипации в широком диапазоне значений числа Фруда на выходе. Получено хорошее совпадение рассчитанных значений с имеющимися экспериментальными данными. Найдено, что степень турбулентности на выходе оказывает сильное влияние на характеристики струи в ближней области.